

# ***Gaia* Assorted Mass Binaries Long Excluded from SLoWPoKES (GAMBLES): Identifying Wide Binary Pairs with Components of Diverse Mass**

Ryan J. Oelkers<sup>1\*</sup>, Keivan G. Stassun<sup>1,2</sup>, Saurav Dhital<sup>1</sup>

## **ABSTRACT**

Despite the maturity of stellar astrophysics, the formation and evolution of binary star systems still remain key questions in modern astronomy. Wide binary pairs (separations  $> 10^3$  AU) are particularly intriguing because their low binding energies makes it difficult for the stars to stay gravitationally bound over extended timescales. The SLoWPoKES I & II catalogs provided the largest and most complete sample of low-mass, wide binary pairs, creating a testbed for the formation and evolution scenarios of multiple star systems. We present an extension of these catalogs, the *Gaia* Assorted Mass Binaries Long Excluded from SLoWPoKES (GAMBLES). This catalog identifies 1,887 candidate binary pairs, of assorted mass, with typical separations between  $10^3 - 10^{5.5}$  AU ( $0.002 - 1.5$  pc) using the published distances and proper motions from the *Tycho-Gaia* Astrometric Solution and Sloan Digital Sky Survey photometry. We find each pair to have *at most* a false positive probability of 0.05 and therefore a total expectation of 23 false binaries in our sample. We find the largest binary separation to be nearly 5.8 pc, 7 systems with 3 components and identify candidate pairs with possible red giant components. We find  $> 92\%$  of GAMBLES binaries have binding energies larger than theoretical limits and dissipation lifetimes longer than 1 Gyr. Given the large separation between the widest GAMBLES binaries, these objects will require the second *Gaia* data release for confirmation. In any event, we find the distribution of binary separations is clearly bimodal between low mass pairs, corroborating the finding from SLoWPoKES and suggesting multiple pathways for the formation and dissipation of the widest binaries in the Galaxy.

## **1. Introduction**

A wide range of astrophysical studies require an unqualified understanding of the fundamental properties of stars. Diverse topics such as planet, star & galaxy formation, the initial stellar mass function, the distance scale and supernovae are just some examples of areas that benefit from realistic models of star formation and evolution (Stassun et al. 2014; Kenicutt & Evans 2012). Binary star systems are particularly useful to the advancement of these fields because they can provide direct measurements of physical parameters and provide insight into basic star formation process and galactic dynamic evolution (Shaya & Olling 2011).

The formation of binary systems is typically understood to occur during a coeval fragmentation of a giant molecular cloud. While this formation theory can explain the occurrence of binary star system with close separations (Duquennoy & Mayor 1991; Raghavan et al. 2010), the discovery of binary pairs with separations near the typical pre-stellar cores has strained typical formation models (Elliott & Bayo 2016).

---

<sup>1</sup>Vanderbilt University, Department of Physics and Astronomy, Nashville, TN 37235

<sup>2</sup>Fisk University, Department of Physics and Astronomy, Nashville, TN 37208

\*Corresponding author: ryan.j.oelkers@vanderbilt.edu

Particularly interesting are very-wide binary pairs, ( $> 1$  pc separation) which provide a unique opportunity to study the formation, evolution and continued stability of binary pairs with separations too wide to be the result of the fragmentation of a molecular cloud.

The creation and sustainability of wide-separation binaries is increasing difficult to explain with a synoptic formation model. The collapse of progenitor molecular clouds into wide-binary pairs has been hypothesized to be caused by the continued passing of numerous stars through the cloud, supernovae explosions, interactions with other giant molecular clouds or dynamical instabilities within the cloud itself (Wasserman & Weinberg 1987; Palasi 2000; Reipurth & Mikkola 2012). The wide separation of these systems, coupled with their immense orbital periods and the large timescale of dynamical interactions, prohibit a comprehensive study of a given system’s orbital parameters through direct observation. Thus, wide binary formation and evolution theory is required to be developed through the inference of the properties from the investigation of large-scale population statistics. This has proven to be a difficult task, given the dearth of confirmed wide-binary pairs with both measured distances and proper motions (Kouwenhoven et al. 2010; Elliott & Bayo 2016).

Recent technological advances have allowed a massive amount of astronomical data to be collected and reduced on practical timescales. Large time-series surveys, such as the Sloan Digital Sky Survey (hereafter SDSS) (York et al. 2000) and the Two-Micron All Sky Survey (hereafter, 2MASS) (Skrutskie et al. 2006), have provided some of the most exquisite astronomical data during the past two decades. The data products from these surveys have permitted massive data mining studies to discover underlying population characteristics and have answered many unresolved questions in Galactic evolution, extra-galactic formation and stellar theory.

The Sloan Low-mass Pairs of Kinematically Equivalent Stars (SLoWPoKES) I & II catalogs (hereafter SLW I & II) provided the largest, statistically significant sample of wide binary pairs to date (Dhital et al. 2010, 2015) and complimented similar studies of wide binary pairs (Sesar et al. 2008). These catalogs were the result of a massive search of the SDSS dataset to identify and characterize low-mass, wide-binary pairs. These binaries included 1,342 low mass pairs which were identified with positions, distances and proper motions and an additional 105,537 pairs identified solely with positions and astrometry. While groundbreaking, these studies were limited by their use of distance-color relations rather than direct distance measurements.

Distance is quite possibly the most fundamental measurable parameter in astronomy but is almost never directly measured. The mission of the *Gaia* space satellite is an ambitious survey with the goal of making a precise 3D map of nearly 100 billion stars over the course of the five year mission lifetime. Following in the footsteps of previous space based astrometric surveys, the satellite will return trigonometric parallax measurements of stars and provide direct distance determinations (van Leeuwen 2007; Lindegren et al. 2016). The first data release provided parallax measurements for stars matched between the *Gaia* data set and the Tycho-2 catalog (Høg et al. 2000; Lindegren et al. 2016).

In this publication we identify systems previously excluded in the SLoWPoKES sample, high to medium mass wide binary pairs. We use the proper motions, parallaxes and positions from the first *Gaia* data release, combined with the photometry, astrometry and proper motions from SDSS to identify binary pairs between multiple Tycho-2 stars and between Tycho-2 and SDSS point sources. We call this extension of the SLoWPoKES catalog the *Gaia* Assorted Mass Binaries Long Excluded from SLoWPoKES (GAMBLES).

The remainder of this paper is organized in the following way: § 2 describes the archival data; § 3 describes our search for binary candidates; § 4 describes our candidate confirmation through the use of a 5D

Galactic Model; § 5 describes our results; § 6 is a discussion of our results; and § 7 are our conclusions.

## 2. Survey Data

### 2.1. Gaia

The *Gaia* spacecraft was launched in December 2013 with a 5 year mission to survey the entire celestial sphere to collect trigonometric parallaxes for more than 100 billion stars. The telescope is expected to achieve an astrometric precision of  $20\mu\text{as}$  or better for all stars with visual magnitudes brighter than  $V \approx 15$  (van Leeuwen 2007; Lindegren et al. 2016).

The satellite has three main instruments: the astrometric field, blue and red photometers and a radial velocity spectrometer. The astrometric field records white light (3300-10500 Å, G-band) for the astrometric calculations. The blue (3300-6800 Å) and red (64000-10500 Å) photometers produce low-resolution spectra over 62 pixels. The radial velocity spectrometer has a resolution of 11,500 from 8470-8710 Å to cover the calcium triplet and provide radial velocities for stars brighter than  $V \approx 16$ . The satellite is covered in 106 CCDs, making a nearly a Gigapixel camera. The spacecraft has two telescopes, each with a field of view of 0.25 sq. degrees, which rotate allowing for every source to be observed 72 times over the course of the 5 year mission (van Leeuwen 2007; Lindegren et al. 2016).

The first data release from the survey provided positions, proper motions and parallaxes for  $\sim 2 \times 10^6$  *Tycho-2* stars and  $\sim 9 \times 10^5$  *Hipparcos* stars to create the *Tycho-Gaia* Astrometric Solution catalog (hereafter, TGAS) (ESA 1997; Høg et al. 2000; van Leeuwen 2007; Lindegren et al. 2016). This catalog is primarily composed of stars with  $V < 11.5$ , contains typical uncertainties of 0.3 mas in the determined positions and parallaxes and  $1 \text{ mas yr}^{-1}$  for the proper motions. Positions for more than  $10^9$  stars were also released in *Gaia*’s secondary data set. Future data releases are expected to include 5 parameter astrometric solutions for all stars determined to be in single star systems, followed by solutions for multiple star systems and culminating in a final data release in 2022.

We have chosen to incorporate the TGAS sample into the SLoWPoKES catalog for 3 reasons. First, the distances provided by the TGAS sample were directly measured through parallax and do not rely on the SDSS distance-color relations from previous SLoWPoKES work (Dhital et al. 2010, 2015). Second, these objects were excluded from the original catalog because the faint limit of the TGAS sample,  $V \approx 12$ , is saturated in the SDSS photometry. Finally, by including this catalog we can search for assorted mass binaries between a variety of spectral types, to probe a regime not yet studied in the SLoWPoKES sample. Incorporating the TGAS catalog allows us to create the GAMBLES catalog.

### 2.2. SDSS

The Sloan Digital Sky Survey (SDSS) is one of the most influential surveys in modern astronomy. The survey, currently on its thirteenth data release (DR-13) (SDSS Collaboration et al. 2016), marked the beginning of the big-data science era in astronomy and shepherded the future of many wide-field surveys such as the Large Synoptic Survey Telescope (LSST) (Ivezic et al. 2008) and the Transiting Exoplanet Survey Satellite (TESS) (Ricker et al. 2014). The survey data has been collected by the 2.5 m telescope at the Apache Point Observatory since the year 2000 (York et al. 2000). The telescope has a 120 mega-pixel camera with a field of view of 1.5 sq. degrees and conducts photometric observations in five optical broad

bands, *ugriz*, between 3000 and 10000 Å.

SDSS DR-13 contains more than 450 million unique objects over the entire 14,555 sq. degrees of the survey which spans the entire Northern sky and the Southern galactic cap. The recalibration of the imaging data has allowed for a decreased systematic uncertainty of  $< 0.9\%$  in *griz* (SDSS Collaboration et al. 2016). As in SLW I & II, we used the Catalog Archive Server query tool (CasJobs) and the SciServer Compute python application to query within radial areas of each *Tycho-2* star in TGAS, to select the sample of possible companions from SDSS.

### 3. Identifying Wide Binary Candidates

The SLW-I& II catalogs were the result of an extensive search for wide separation binaries in the SDSS dataset, which we extend in GAMBLES to include TGAS. While the final GAMBLES sample is a single catalog, it was formed in two distinct parts. The search of SDSS point sources for companions to the TGAS catalog and a search for wide binaries within the TGAS sample.

#### 3.1. SDSS Query

We queried the SDSS DR-13 using CASJobs within  $3'$  of each Tycho-2 position using the STAR, PROPERMOTIONS and TWOMASS tables in CasJobs to create our first data subset (hereafter, TGAS-SDSS). We applied cuts to this initial search sample for two reasons. First, the large number of TGAS stars and SDSS matches within the SDSS footprint, allowed us to select only the best candidates and exclude the objects with poor photometry and proper motions. Second, a large majority of stars queried within a  $3'$  radial search are *not* likely to be *bona-fide* binaries but only chance alignments. These cuts are described below.

First, we removed stars from the search based on the following quality flags for *riz*, requiring all to be zero: PEAK\_CENTER, NOTCHECKED, PSF\_FLUX\_INTERP, INTERP\_CENTER, BAD\_COUNTS\_ERROR, SATURATED, BRIGHT, NOBLEND and DELEND\_NOPEAK. We only required these cuts on the *riz* magnitudes because these were the magnitudes we used to identify varying spectral types and distances. Second, we set limits on the size of the residual difference between the *riz* point-spread-functions (hereafter, PSF), requiring  $PSFMAG_r - PSFMAG_i \geq 0.30$ ,  $PSFMAG_I = PSFMAG_Z \geq 0.20$ . Third, we required each PSF to be larger than 0 with the absolute value of the uncertainty to be less than 0.1 mag. Finally, we required the extinction in *r* to be less than 0.5 magnitudes and for the proper motion be larger than  $40''$ . This search resulted in 195,212 candidate secondaries from the SDSS catalog for 136,969 TGAS stars.

We included the following 2 cuts to further constrain our sample and only include stars most likely to be in binary pairs based on kinematics:

1.  $\Delta d < \min(0.1383\sqrt{d_1^2 + d_2^2}, 100 \text{ pc})$ , where  $d$  is the distance in pc with  $d_1$  and  $d_2$  representing the distances to the two components.
2.  $\sqrt{(\frac{\Delta\mu_{RA}^2}{\sigma_{\mu_{RA}}}) + (\frac{\Delta\mu_{Dec}^2}{\sigma_{\mu_{Dec}}})} < 2$ , where  $\mu$  is the proper motion.
3.  $d_\mu > d_\sigma$  where  $d_\mu$  is the mean distance of the pair and  $d_\sigma$  is the combined error of the distances.

The addition of these cuts created our final TGAS-SDSS sample which included 281 candidate pairs.

### 3.2. Distances with SDSS Photometry

We estimated the distance to SDSS candidate objects, following the procedure from previous SLoW-PoKES work, by using SDSS photometric colors (Dhital et al. 2010, 2015). For stars assumed to be on the main sequence, whose colors did not match a sub-dwarf or white dwarf, we use the relation from Covey et al. (2007). For stars with main-sequence colors that match K5 to M9 we use the relation from Bochanski et al. (2010). We estimated the distances for stars with colors matching spectral types later than M9 using the relation from Schmidt et al. (2010).

For stars whose colors match those of subdwarfs, we use the relation from Bochanski et al. (2012). We calculate the distance to stars with the colors of white dwarfs using *ugriz* photometry and the Bergeron et al. (1995) models. These models use a chi-square minimization technique and assume a hydrogen dominated atmosphere. Any star without a color matching to the above categories was removed from our sample.

### 3.3. Gaia Query

We similarly queried TGAS with a radial search of 3' around each TGAS star to identify wide binary candidates (this sample is hereafter, TGAS-TGAS). We similarly constrained our TGAS-TGAS sample by the 3 kinematic constraints mentioned in § 3.1. These constraints led to 5,842 candidate pairs.

As described above, the TGAS stars have their distances measured directly using trigonometric parallaxes from the *Gaia* satellite (Lindgren et al. 2016). We use the normal formula to convert from parallax to distance  $d = \frac{1}{\pi}$ , where  $\pi$  is measured in arcseconds and  $d$  is measured in parsecs.

#### 3.3.1. SDSS Photometry for Tycho-2 Stars

While many stars in the TGAS sample never had SDSS *ugriz* observations (at least not in a comprehensive, systematic way), we elected to use the synthetic SDSS photometry provided by Pickles & Depagne (2010) to estimate each spectral type. These magnitudes were created by fitting the  $B_T$ ,  $V_T$  and 2MASS  $JHK$  magnitudes to interpolate to the SDSS filters. We adopt the photometric uncertainties as (0.2, 0.06, 0.04, 0.04, 0.05) in *ugriz* respectively, based on the uncertainties provided in Pickles & Depagne (2010). We estimated the extinction to each star using the 3D dust map from Bovy et al. (2016) and the TGAS distances. This dust map combines previous Galactic extinction calculations from Drimmel et al. (2003), Marshall et al. (2006) and Green et al. (2015) to provide one of the most comprehensive estimates of Galactic extinction to date.

We then used the same relations described in § 3.1 to determine a photometric spectral type using the synthetic magnitudes and calculated extinction. Stars which did not fall into the color ranges provided by these relations were not assigned a spectral type but were included in our sample since the distances were based on trigonometric parallax and not dependent on a color based relation.

#### 4. Assessing False Positive Likelihood with a Galactic Model

The cuts described in § 3 provide a sample of candidate wide binary pairs but provide little evidence to the authenticity of each pair. Consequently, many of these candidates are due to chance alignments. While the inclusion of the *Gaia* parallaxes helps to alleviate this tension, the uncertainties in the parameters used to determine the SDSS color based distances do not completely remove ambiguity. This is particularly important for pairs with large angular separation.

Similar to previous SLoWPoKES work, we employ a 5-dimensional model to recreate the stellar populations along a given line of sight and calculate the probability of a chance alignment. This model applies the empirically measured parameters of the Milky Way to account for stellar number density and spacial velocities to assess the chance of alignment probability. We provide a brief summary of the model below and direct the reader to Dhital et al. (2010) for a more detailed explanation.

An ideal model Galaxy would be simulated with  $10^{11}$  stars based on the number density and population of the Milky Way each with a unique position, proper motion and radial velocity. However, given the enormous computational resources required for such a simulation, our model instead simulates a cone, centered at the  $(\alpha, \delta)$  of each TGAS source out to a distance of 2.5 kpc. The stellar number density in the cone is calculated by integrating the Galactic density profiles and assumes a bimodal disk with an ellipsoidal halo. The line of sight is repopulated with stars using a rejection method to ensure a random redistribution using the previously calculated stellar density. For the binary stars in the GAMBLES sample, typically between 150 and 15,000 stars were generated along a given line of sight for each  $\alpha, \delta$  and distance. While this two-dimensional model is adequate for our needs we stress it is an oversimplification of the Galactic scale height and does not reproduce local variation such as moving groups or clusters.

We then ran an ellipsoidal search, defined by the angular separation, distance errors and proper motions of a given pair, to simulate our SDSS and TGAS searches described above. 1,000 Monte-Carlo realizations were run for each pair. We divided the total number of stars along a given line of sight, with matching characteristics to our candidate binaries, by the total number of Monte-Carlo realizations to determine how likely a given binary pair was due to a chance alignment.

We stress that this metric is not a formal probability but instead an estimate on the number density of stars with similar characteristics in a given 5-D Voxel (hereafter,  $V_5$ ). Stars which returned a value of  $V_5 = 0$  (i.e.  $< 1$  in 1000 stars) were assigned  $V_5 = 0.001$  because their true  $V_5$  was below the resolution of our Monte-Carlo procedure. We selected candidate pairs which return a value of  $V_5 \leq 0.05$  as *bona-fide* wide binary pairs following previous SLoWPoKES work (Dhital et al. 2010, 2015).

#### 5. Results

Our cut of  $V_5 \leq 0.05$  produced 2,325 statistically significant wide-binary pairs with separations of  $10^3 - 10^6$  AU: 206 out of 281 pairs in the TGAS-SDSS sample and 2119 out of 5838 pairs in the TGAS-TGAS sample. Figure 1 shows photographic cut-outs of SDSS & 2MASS images for 9 statistically significant wide-binary pairs. Table 1 provides the properties for each binary in the GAMBLES sample.

Figure 3 shows all binary candidates we subjected to the Galactic Model and their resulting  $V_5$  values. We find most candidate binaries show a high  $V_5$  ( $V_5 \gg 0.05$ ) at very large angular separations,  $\sim 140 - 180''$ . This is not surprising given that, at high angular separations, candidate pairs are more susceptible to being a chance alignment. The large number of pairs with small angular separations and low values of  $V_5$  are due

to the resolution of our Galactic Model being 0.001.

We also searched the GAMBLES sample for possible systems with more than 2 components. We did this by comparing the primary and secondary stars of each binary to look for pairs with matching primaries or secondaries. We found 7 systems where the primary was linked to more than 1 secondary object.

We will upload the GAMBLES catalog, including the objects which did not pass our Galactic Model, to the FILTERGRAPH portal (Burger et al. 2013). This allows the catalog to be easily accessible to the astronomical community, will allow for transparency in our sample and provide ease of access for any follow up observations to confirm the authenticity of each binary pair.

### 5.1. Distribution of Binary Pair Separations

The 1,342 SLW-I and 105,537 SLW-II binary pairs were found to have separations between  $10^3 - 10^5$  AU. The GAMBLES sample of 2,325 assorted mass binaries greatly extends the SLoWPoKES sample to separations of  $10^6$  AU. While the distributions of binary pairs in our TGAS-SDSS sample is "tight" with separations of 2,500 – 40,000 AU, we find the TGAS-TGAS sample to be much broader with separations ranging from 600 – 95,000 AU or 0.003 – 5.76 pc

We find the TGAS-SDSS sample has a bimodal distribution with a peak at  $\sim 10^4$  and  $\sim 10^{4.75}$ , as shown in Figure 6. Interestingly, this is nearly identical to the SLW-I bimodal distribution which had peaks near  $10^{3.6}$  and  $10^{4.7}$  AU and greatly reinforces the interpretation that multiple wide-binary populations exist in the Galaxy, with each peak representing a binary population which forms and dissipates using a unique methods (Dhital et al. 2010).

While the TGAS-TGAS sample does not show a bimodal distribution, it has a skewed distribution with the left tail falling much more slowly than the right tail. We find the distribution can be fit well with a single, power-law polynomial as shown in Figure 5 with the peak of the distribution found near  $10^{4.75}$  AU. We find the majority of GAMBLES binaries in the TGAS-TGAS sample have wider separations,  $> 10^{3.5}$  AU, than the SLW-I & II samples, with the peak falling to the right of the SLW-II sample but aligning quite nicely with the SLW-I second bimodal peak. This likely implies the TGAS-TGAS sample is primarily composed of stars within a single type of wide binary population.

Perhaps most interestingly, the TGAS-TGAS sample also contains 248 very wide binaries (see Figure 7) with separations larger than 1 pc. If these systems are truly gravitationally bound, they would represent some the widest binary pairs known. We discuss the implications of the widest binaries and the likelihood of their *bona-fide* nature in § 6.2.

Given the large separation between of the TGAS-TGAS components,  $> 3$  pc in some cases, it would be reasonable to assume there could be interloper stars between the two components which could disrupt the pairs. We searched each of the 206 binary pairs from the TGAS-SDSS sample, and all stars in the TGAS-TGAS sample within the SDSS footprint, for stars at similar distances but did not share similar proper motions or failed the  $V_5$  statistical cut. We found 10 binaries to also have a star with a similar distance where the separations between the components is between  $10^{3.8} - 10^{4.7}$  AU. From this analysis we expect  $< 4\%$  of the GAMBLES sample to be affected by a possible interloper star during its lifetime.

## 5.2. Distribution of Binary Component Types

We categorized the 2,325 assorted mass binary pairs into a basic class and spectral type using the color relations described in § 3. Each star was assigned a spectral type, O to M, and given a basic classification: main-sequence (MS), very-low mass (VLM), white dwarf (WD) or sub-dwarf (sdM). We also assigned a spectral type to each binary component if the stellar colors,  $r - z$ , were within the acceptable ranges. We find we recover binary component spectral types from O to M. Additionally, we found at least 1 binary pair primary, with spectral type of A or later, to match to an M dwarf secondary.

We stress, however, that this spectral typing has been based on photometry alone and there could be some miss-classifications. This is particularly important in the case of the stars in the TGAS catalog where the photometry is synthetic rather than observed. These categorizations are not statistically scrutinized by our Galactic Model and we cannot quantify their integrity without proper photometric and spectroscopic follow-up. However, these categorizations passed each of our imposed color cuts and we have kept the designations in the final GAMBLES catalog.

## 6. Discussion

While the Galactic Model does a proficient job of determining chance alignment probabilities in 5 dimensional space, it does not qualify binary likelihood based on the physical properties of each system. It is critical we address the practicality of many of these systems, particularly the systems with separations  $> 1$  pc or at heliocentric distances  $> 2.5$  kpc where our Galactic model does not adequately represent the full volume in a given 5-D voxel.

Given the large separation of widest binaries in the GAMBLES sample (see Figure 7), we wanted to objectively test the validity of their separations. This objectivity is particularly important for the statistical nature of our selection because we cannot simply exclude a binary pair because the component separation appears implausible but the pair alignment is statistically significant.

We further investigate the authenticity of each binary pair in three ways. First, we compare the GAMBLES sample to previous wide binary samples to find similarities in the binary separations and investigate underlying sample populations. Second, we calculate the binding energies of each pair to place a realistic constraint on the furthest separation each binary is physically capable of. And third, we determine the expected dissipation lifetimes of each pair to understand their future gravitational stability.

### 6.1. The Diversity of the GAMBLES Sample

As previously stated, the SLW-I catalog identified a bimodal distribution at  $10^{3.6}$  and  $10^{4.7}$  AU. This was interpreted as a combination of separate wide binary populations in the Galaxy and evidence of varying formation and evolutionary methods for differing binary populations (Dhital et al. 2010). The bimodal peak at  $10^{4.7}$  AU was proposed to represent a population of binary pairs which are loosely bound after the dissipation of the main star forming cluster. This hypothesis was reinforced by the size of a typical pre-stellar core matching the separations of many of the candidate binaries ( $\sim 0.35$  pc or  $\sim 10^{4.9}$  AU (Kouwenhoven et al. 2010)). The bimodal peak at  $10^{3.6}$  AU could represent a population of wide binaries which formed together in the same molecular cloud but migrated outwards due to dynamic instability, which has been shown in recent work (Reipurth & Mikkola 2012; Elliott & Bayo 2016). While the SLW-II catalog

did not recover a bimodal distribution in its binary population it found its population was best described with the combination of two power law functions likely, due to varying combinations of the above described populations (Dhital et al. 2015).

The GAMBLES catalog shows both similarities and differences to the previous SLoWPoKES catalogs. By separating the two samples in the GAMBLES catalog, TGAS-TGAS and TGAS-SDSS, we see distinct features in the populations. As shown in Figure 6, the population of the TGAS-SDSS sample is strikingly similar to the SLW-I sample with peaks in the population at  $10^4$  and  $10^{4.75}$  AU. We find these binary pairs to be almost entirely lower mass object with the spectral types of the primary stars ranging from A-K and the secondaries ranging from G-M. These similarities seem to suggest that low mass pairs are susceptible to forming in systems either through outward migration or loosely bound capture.

The population of binaries from the TGAS-TGAS sample does not show a bimodal distribution and is fit well with a single power-law polynomial as shown in Figure 5. This single power-law fit is a departure from previous SLoWPoKES analysis which found a break in the power-law distribution near separations of  $10^{3.75}$  AU.

Interestingly, the peak of the distribution is found to be near  $10^{4.7}$  AU and matches the TGAS-SDSS bimodal peak. This could suggest that higher mass wide binaries are more likely to form by loosely bound capture after the dissipation of the star cluster as noted above given the average combined mass of the TGAS-TGAS sample is  $\sim 3.2M_{\odot}$ . Additionally, We find evidence of a slight separation near the split in the peaks of the TGAS-SDSS sample (shown with an orange arrow in Figure 5) suggesting the bimodal distribution is not observed in the TGAS-TGAS sample because is not a 1 dimensional relationship and the peaks are being smeared together at higher mass as shown in Dhital et al. (2010).

## 6.2. Analyzing the Fidelity of the Widest Binaries in GAMBLES

### 6.2.1. Binding Energies of the GAMBLES Sample

Our Galactic model provides an expected number density of stars along a given 5-D voxel of positions, distances and proper motions. While the model provides sufficient evidence against the chance alignment of similar stars, especially out to heliocentric distances of  $< 2.5$  kpc, there could still be impostors in our sample. Many of the GAMBLES binary separations also appear to break previously observed empirical limits on wide binary separations (Reid et al. 2001; Close et al. 2003; Burgasser et al. 2003; Close et al. 2007). However, if these pairs retain adequate gravitational binding energy over their large separation, then they could be still considered to be *bona-fide* wide separation binaries.

Previous studies have proposed empirical limits on binding energies of wide binaries to be  $10^{40}$  for sub-stellar objects,  $10^{41}$  ergs for stars and  $10^{42.5}$  for the lowest mass objects (Reid et al. 2001; Close et al. 2003; Burgasser et al. 2003; Close et al. 2007). We calculated the binding energies of the GAMBLES sample to quantify the physicality of many of our widest pairs. We define the binding energy of a binary pair, measured in ergs, as the gravitational potential energy between the two objects:

$$U = -\frac{GM_1M_2}{r}$$

where  $G$  is the gravitational constant,  $M_1$  and  $M_2$  are the masses of each binary component and  $r$  is the distance between the two stars. Figure 8 shows calculated binding energies for each binary where a  $r - z$

color was available to estimate a given component’s mass.

While all stars from the SDSS sample were required to have a suitable  $r - z$  color, the distances for the TGAS stars were defined using the observed *Gaia* trigonometric parallaxes and SDSS colors were therefore, not required. While we used the synthetic photometry of (Pickles & Depagne 2010) to estimate stellar mass, not all stars in TGAS had available synthetic photometry. We have elected to remove 438 binaries from the sample which could not have their mass, and thus their binding energies, estimated. After imposing this cut we have 1,887 binaries which we accept as the final GAMBLES sample.

We summed the expected false positive values for these 1,887 binaries and found the expected number of false positive binaries to be  $\Sigma V_5 = 22.725$ . This number is not significant enough to significantly change our binary population even at very wide separations,  $d > 1$  pc.

Figure 10 shows  $H_g$  vs.  $g - i$  for the GAMBLES sample. These reduced proper motion diagrams can provide useful insight into the nature of common proper motion binaries and have been used previously to identify candidate pairs (Chanamé & Gould 2004; Dhital et al. 2010). The top part of Figure 10 shows reduced proper motion diagrams for the GAMBLES sample and the link between each binary pair.

We used the bolometric flux and effective temperature relations from Casagrande et al. (2010), coupled with the  $B_T$  and  $V_T$  magnitudes, to estimate each stellar radii. If a star was shown to have a radius  $R > 10R_\odot$  we flagged the star as a likely giant. We identified 467 candidate binary pairs where at least 1 star had an estimated radius larger than  $10R_\odot$ . While these binary pairs will have a decreased binding energy (see bottom panel of Figure 10), if these giant components are in *bona-fide* wide-binary pairs they would represent the first known systems with evolved components.

If we impose a hard limit of  $10^{41}$  ergs we find that 139 of the binaries with calculable masses fall below this limit. The fact that these binaries have binding energies below what is expected, but are statistically significant in our Galactic Model, has a few implications. The first is that the population of binaries which fail the cut are dynamically unstable and are drifting apart but retain some characteristics of the initial system (such as similar proper motions).

The second implication could be that the previous empirical limits were too conservative for the widest binary pairs. Given recent work in the detection of wide-binaries this may not be implausible. The SLW I & II samples found nearly the entire catalog violated these empirically imposed limits, with binding energies closer to that of Neptune and the Sun at  $10^{40}$  ergs. This suggested the limits on binding energy could have been too conservative for the widest separation objects (Dhital et al. 2010, 2015). Similarly, recent work by Semyeong et al. (2016) identified 13,085 common proper motion pairs in the TGAS data set, many with separations  $> 3$  pc. While it is likely these pairs are not wide-binaries, these stars likely trace larger moving groups and open clusters such as Upper Scorpius and the Pleiades in the Galaxy. Given the wide separation of these objects, it is possible the GAMBLES sample contains remnants of former moving groups.

The third implication is that these binaries have low binding energies because they are not *bona-fide* binaries. This last interpretation is strengthened by the caveat that our Galactic Model does not reproduce the Galactic stellar distribution past  $\sim 2.5$  kpc and the widest statistically significant GAMBLES binaries (separations  $> 2$  pc) are found to be at heliocentric distances of  $2 - 7$  kpc. We address these concerns in § 6.2.2.

### 6.2.2. The Dissipation Lifetimes of the GAMBLES Sample

Even if a binary pair possesses the requisite binding energy to remain stable, the large separation coupled with the local Galactic environment could cause the pair to dissipate over time. Encounters with other stars, molecular clouds or even subtle changes in the overall Galactic potential can combine to disrupt the system’s stability and cause it to break apart (Weinberg et al. 1987). We calculated the average dissipation lifetime of a given binary to aid in our interpretation of the possible stability of each system. We followed the logic of Weinberg et al. (1987); Close et al. (2007); Dhital et al. (2010) and used the below approximation, based on the advection and diffusion of orbital binding energy due to small encounters, to calculate the expected dissipation lifetimes:

$$a \approx 1.212 \frac{M_{tot}}{t_*}$$

where  $a$  is the separation in pc,  $M_{tot}$  is the total mass of the system in solar masses and  $t_*$  is the lifetime of the binary in Gyr. Figure 9 shows the binding energies and separations of each statistically significant GAMBLES pair with the over-plotted dissipation lifetimes of 1, 10 and 100 Gyr.

We find no GAMBLES binary has a dissipation lifetime shorter than 1 Gyr and a binding energy of  $< 10^{41}$  ergs. Our widest binary pair, with a separation of  $\sim 5.76$  pc, has a lifetime of 1.13 Gyr. Given the photometric spectral types of the pair, B9 & A0, the pair must be quite young. The main sequence lifetime of a late B and early A star is  $\sim 0.5$  Gyr which implies this pair will likely be stable for the entire main-sequence lifetime of both stars.

We find the widest binaries ( $> 1$  pc) in our sample have expected lifetimes  $< 10$  Gyr. However, when this information is coupled with their photometric spectral types (ranging from O to G) we find these stars are both young and likely stable through their main sequence lifetimes. Interestingly, because we find a diverse population of stellar masses in our binary pairs, we also find a diverse set of lifetimes, even at large separations. For example, out to  $10^5$  AU we find dissipation lifetimes in our sample from  $< 10$  to  $> 100$  Gyr.

## 7. Conclusions

We have extended the SLoWPoKES catalog to include high to medium mass wide binary candidates using the Sloan Digital Sky Survey photometry and parallaxes and proper motions from the *Tycho-Gaia* Astrometric Solution. Our analysis has discovered 1,887 assorted mass binaries, with component spectral types ranging from O to M and separations between  $10^3$ – $10^6$  AU. This data set provides a unique opportunity to study a population of binary stars that is diverse in spectral type and separation.

Our analysis included the comparison of position, distance, angular separation, proper motions, binding energies and dissipation lifetimes to reduce the number of false positive candidates. We employed a Galactic Model, combined with a Monte Carlo analysis, to determine the expected number of similar stars along a given line of sight. We removed any binary pair from our sample where the number of similar stars per line of sight was  $> 5$  in 1000. We also excluded any binary star where a mass could not be estimated.

We find the GAMBLES sample is split into two populations of wide separation binaries. The first group, with separations near  $10^4$  AU likely formed through outward migration due to dynamic instabilities. The second, with separations near  $10^{4.75}$  AU, likely formed through weak gravitational interactions after cluster

dissipation. Our results corroborate previous SLoWPoKES work which found a bimodal distribution of wide binaries and hint at a possible relationship between component mass, binary separation and dissipation lifetime driving the formation and evolution of these systems.

Finally, the GAMBLES catalog will be available on the Filtergraph portal (Burger et al. 2013). This web-based service allows for open source access to many datasets and provides fast plotting and filtering features useful in determining data trends and visualizing large data sets.

This work has made use of data from the European Space Agency (ESA) mission *Gaia* (<http://www.cosmos.esa.int/gaia>) processed by the *Gaia* Data Processing and Analysis Consortium (DPAC, <http://www.cosmos.esa.int/web/gaia/dpac/consortium>). Funding for the DPAC has been provided by national institutions, in particular the institutions participating in the *Gaia* Multilateral Agreement. This work has made extensive use of the Filtergraph data visualization service (Burger et al. 2013) at <http://www.filtergraph.vanderbilt.edu>. This research has made use of the VizieR catalogue access tool, CDS, Strasbourg, France. This work was conducted in part using the resources of the Advanced Computing Center for Research and Education at Vanderbilt University, Nashville. Funding for the Sloan Digital Sky Survey IV has been provided by the Alfred P. Sloan Foundation, the U.S. Department of Energy Office of Science, and the Participating Institutions. SDSS-IV acknowledges support and resources from the Center for High-Performance Computing at the University of Utah. The SDSS web site is [www.sdss.org](http://www.sdss.org). SDSS-IV is managed by the Astrophysical Research Consortium for the Participating Institutions of the SDSS Collaboration including the Brazilian Participation Group, the Carnegie Institution for Science, Carnegie Mellon University, the Chilean Participation Group, the French Participation Group, Harvard-Smithsonian Center for Astrophysics, Instituto de Astrofísica de Canarias, The Johns Hopkins University, Kavli Institute for the Physics and Mathematics of the Universe (IPMU) / University of Tokyo, Lawrence Berkeley National Laboratory, Leibniz Institut für Astrophysik Potsdam (AIP), Max-Planck-Institut für Astronomie (MPIA Heidelberg), Max-Planck-Institut für Astrophysik (MPA Garching), Max-Planck-Institut für Extraterrestrische Physik (MPE), National Astronomical Observatories of China, New Mexico State University, New York University, University of Notre Dame, Observatório Nacional / MCTI, The Ohio State University, Pennsylvania State University, Shanghai Astronomical Observatory, United Kingdom Participation Group, Universidad Nacional Autónoma de México, University of Arizona, University of Colorado Boulder, University of Oxford, University of Portsmouth, University of Utah, University of Virginia, University of Washington, University of Wisconsin, Vanderbilt University, and Yale University. We acknowledge use of the ADS bibliographic service.

## REFERENCES

- Bergeron, P., Wesemael, F., & Beauchamp, A. 1995, *PASP*, 107, 1047
- Bochanski, J. J., Hawley, S. L., Covey, K. R., et al. 2010, *AJ*, 139, 2679
- . 2012, *AJ*, 143, 152
- Bovy, J., Rix, H.-W., Green, G. M., Schlafly, E. F., & Finkbeiner, D. P. 2016, *ApJ*, 818, 130
- Burgasser, A. J., Kirkpatrick, J. D., Reid, I. N., et al. 2003, *ApJ*, 586, 512
- Burger, D., Stassun, K. G., Pepper, J. A., et al. 2013, in *Astronomical Society of the Pacific Conference Series*, Vol. 475, *Astronomical Data Analysis Software and Systems XXII*, ed. D. N. Friedel, 399

- Casagrande, L., Ramírez, I., Meléndez, J., Bessell, M., & Asplund, M. 2010, *A&A*, 512, A54
- Chanamé, J., & Gould, A. 2004, *ApJ*, 601, 289
- Close, L. M., Siegler, N., Freed, M., & Biller, B. 2003, *ApJ*, 587, 407
- Close, L. M., Zuckerman, B., Song, I., et al. 2007, *ApJ*, 660, 1492
- Covey, K. R., Ivezić, Ž., Schlegel, D., et al. 2007, *AJ*, 134, 2398
- Dhital, S., West, A. A., Stassun, K. G., & Bochanski, J. J. 2010, *AJ*, 139, 2566
- Dhital, S., West, A. A., Stassun, K. G., Schluns, K. J., & Massey, A. P. 2015, *AJ*, 150, 57
- Drimmel, R., Cabrera-Lavers, A., & López-Corredoira, M. 2003, *A&A*, 409, 205
- Duquennoy, A., & Mayor, M. 1991, *A&A*, 248, 485
- Elliott, P., & Bayo, A. 2016, *MNRAS*, 459, 4499
- ESA, ed. 1997, ESA Special Publication, Vol. 1200, The HIPPARCOS and TYCHO catalogues. Astrometric and photometric star catalogues derived from the ESA HIPPARCOS Space Astrometry Mission
- Green, G. M., Schlafly, E. F., Finkbeiner, D. P., et al. 2015, *ApJ*, 810, 25
- Høg, E., Fabricius, C., Makarov, V. V., et al. 2000, *A&A*, 355, L27
- Ivezic, Z., Tyson, J. A., Abel, B., et al. 2008, ArXiv e-prints, arXiv:0805.2366
- Kennicutt, R. C., & Evans, N. J. 2012, *ARA&A*, 50, 531
- Kouwenhoven, M. B. N., Goodwin, S. P., Parker, R. J., et al. 2010, *MNRAS*, 404, 1835
- Lindgren, L., Lammers, U., Bastian, U., et al. 2016, ArXiv e-prints, arXiv:1609.04303
- Marshall, D. J., Robin, A. C., Reylé, C., Schultheis, M., & Picaud, S. 2006, *A&A*, 453, 635
- Palasi, J. 2000, in *IAU Symposium*, Vol. 200, IAU Symposium, 145
- Pickles, A., & Depagne, É. 2010, *PASP*, 122, 1437
- Raghavan, D., McAlister, H. A., Henry, T. J., et al. 2010, *ApJS*, 190, 1
- Reid, I. N., Burgasser, A. J., Cruz, K. L., Kirkpatrick, J. D., & Gizis, J. E. 2001, *AJ*, 121, 1710
- Reipurth, B., & Mikkola, S. 2012, *Nature*, 492, 221
- Ricker, G. R., Winn, J. N., Vanderspek, R., et al. 2014, in *Proc. SPIE*, Vol. 9143, Space Telescopes and Instrumentation 2014: Optical, Infrared, and Millimeter Wave, 914320
- Schmidt, S. J., West, A. A., Hawley, S. L., & Pineda, J. S. 2010, *AJ*, 139, 1808
- SDSS Collaboration, Albareti, F. D., Allende Prieto, C., et al. 2016, ArXiv e-prints, arXiv:1608.02013
- Semyeong, O., Price-Whelan, A. M., Hogg, D. W., Morton, T. D., & Spergel, D. N. 2016, in-prep
- Sesar, B., Ivezić, Ž., & Jurić, M. 2008, *ApJ*, 689, 1244

- Shaya, E. J., & Olling, R. P. 2011, *ApJS*, 192, 2
- Skrutskie, M. F., Cutri, R. M., Stiening, R., et al. 2006, *AJ*, 131, 1163
- Stassun, K. G., Feiden, G. A., & Torres, G. 2014, *New Astronomy Reviews*, 60, 1
- van Leeuwen, F., ed. 2007, *Astrophysics and Space Science Library*, Vol. 350, *Hipparcos, the New Reduction of the Raw Data*
- Wasserman, I., & Weinberg, M. D. 1987, *ApJ*, 312, 390
- Weinberg, M. D., Shapiro, S. L., & Wasserman, I. 1987, *ApJ*, 312, 367
- York, D. G., Adelman, J., Anderson, Jr., J. E., et al. 2000, *AJ*, 120, 1579

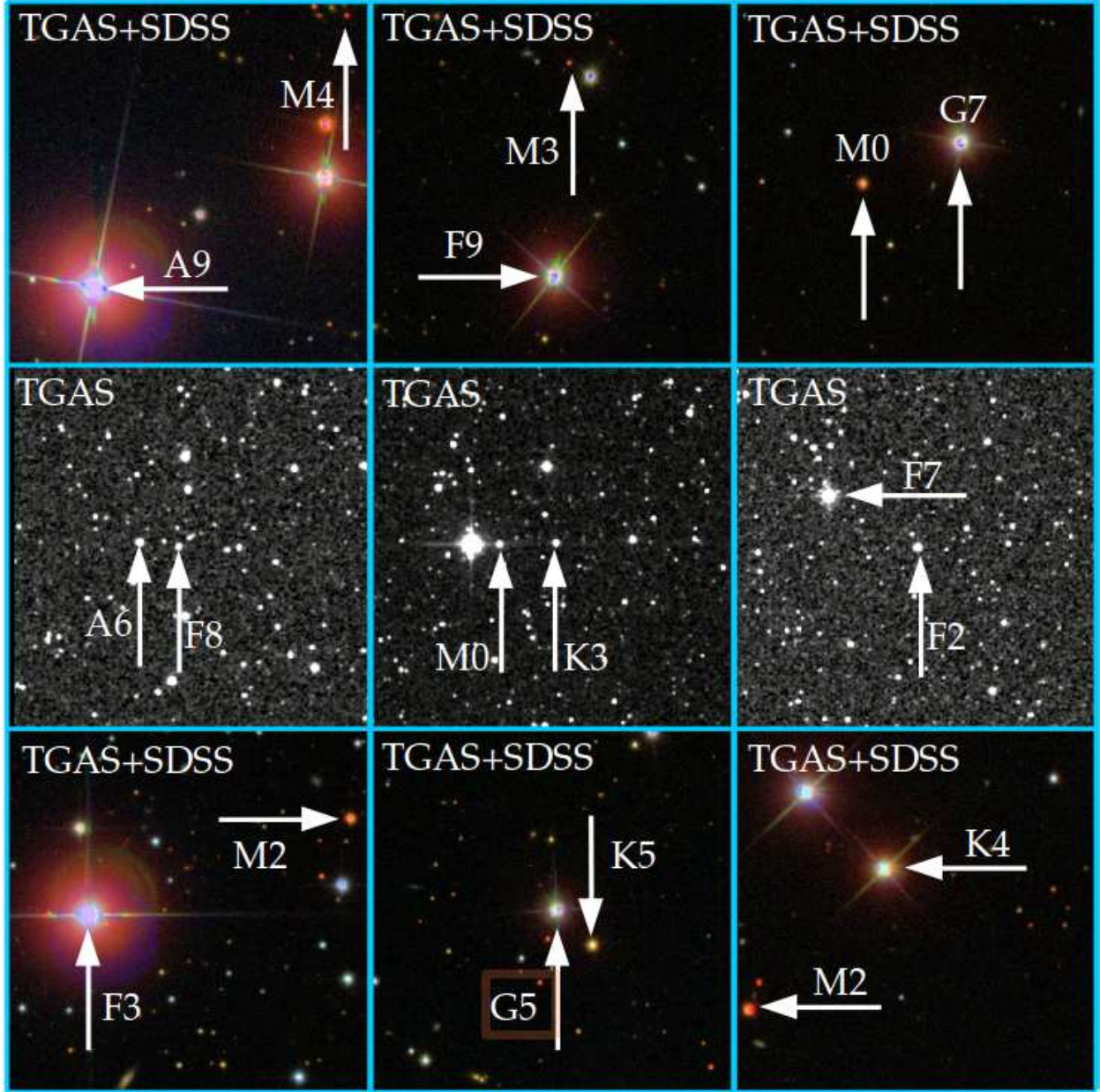


Fig. 1.— SDSS and 2MASS images of 9 selected binaries from the GAMBLES sample of assorted mass. Images from SDSS are  $3'$  on a side while images from 2MASS are  $6'$  on a side. The label on the top left of all frames details whether the pair was discovered by a match between TGAS and SDSS or within TGAS.

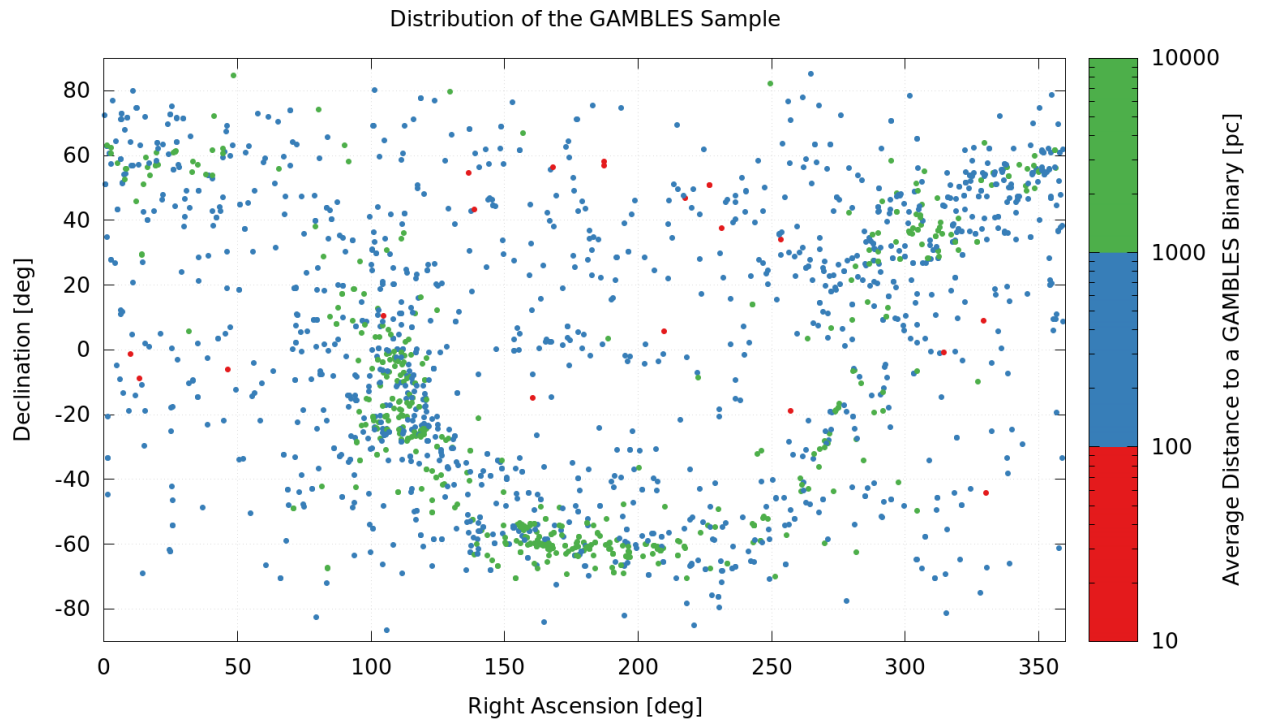


Fig. 2.— An all-sky map of GAMBLES binary stars. *Top*: The map shows the mean position of each binary on the sky in Right Ascension [deg] and Declination [deg]. The color denotes the distance to the binary from the Sun, in pc.

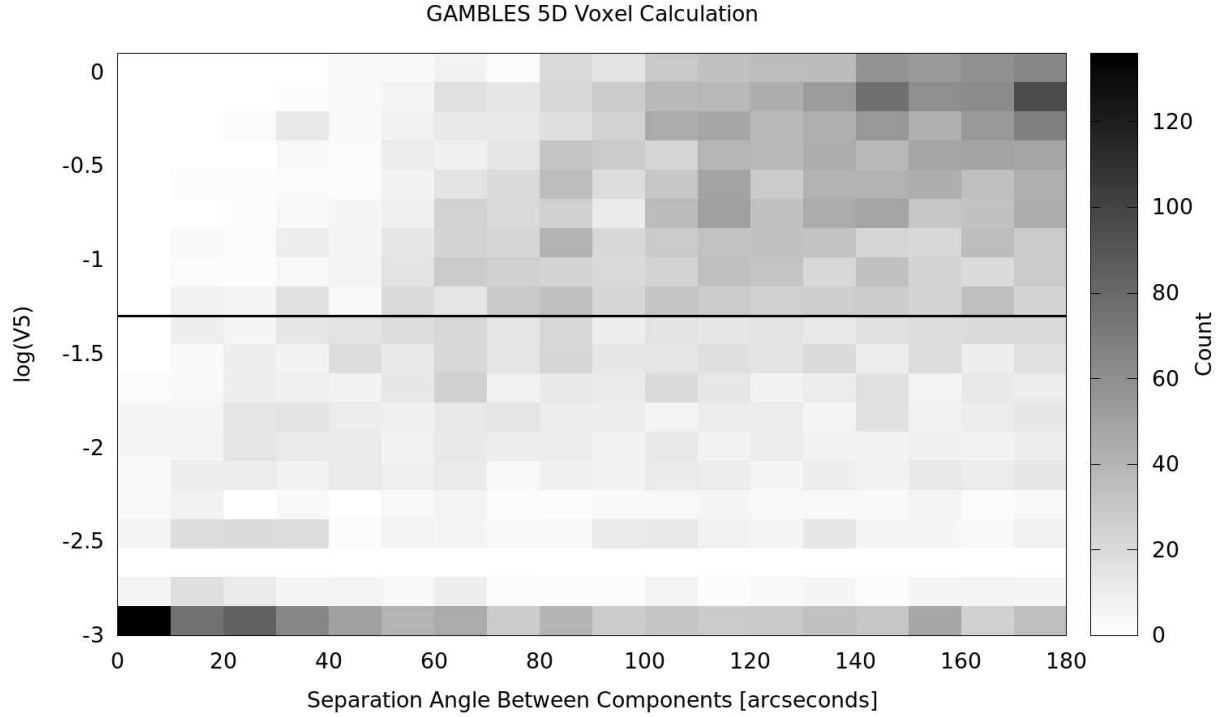


Fig. 3.— A heatmap, in log space, of the  $V_5$  statistic versus the angular separation of each binary pair. Each box is shaded by the number of stars falling in a given area, with the darker boxes containing more stars. Our cut of  $V_5 < 0.05$  is shown as a black line. The number of stars with a high false-alarm value increases as the angular separation increases, as is to be expected. The pile up of stars with low false-alarm probability (0.001) is due to the resolution of our Monte-Carlo simulation being 1 in 1000. Stars with  $V_5$  below 0.001 are all high-confidence pairs.

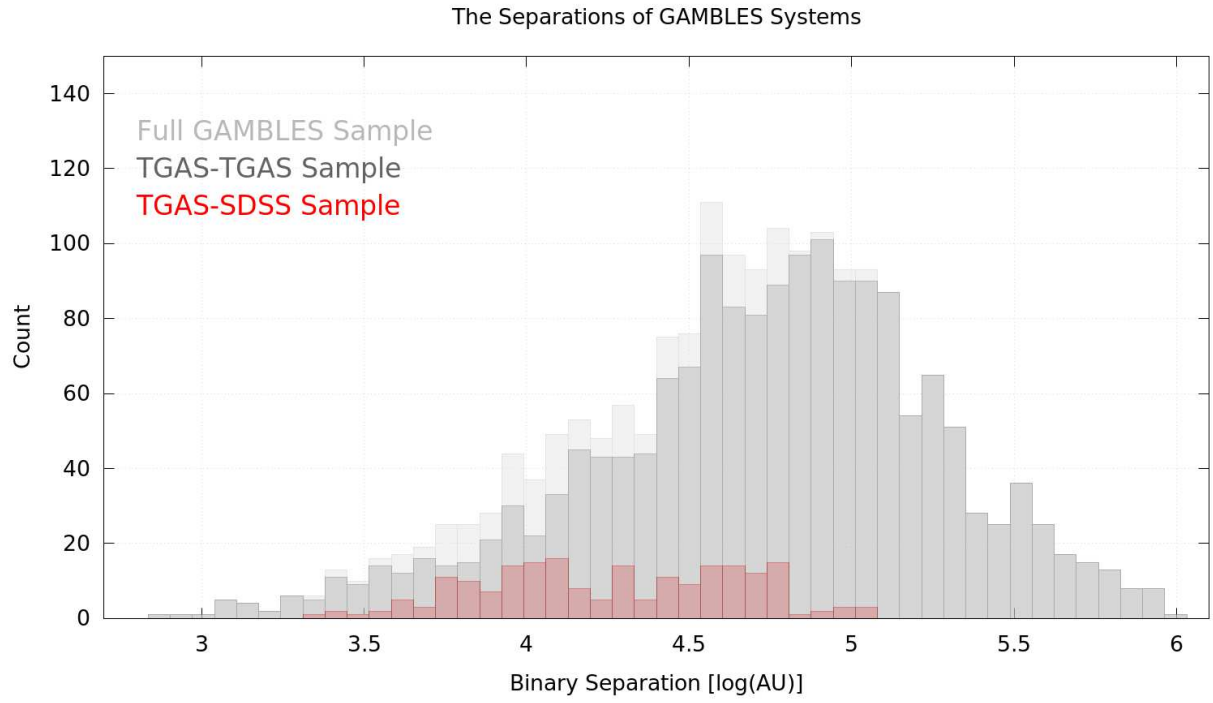


Fig. 4.— The projected separation for GAMBLES binaries in  $\log(\text{AU})$  (*bottom*). We find the majority of the binaries have separations between  $10^3 - 10^5$  AU with 25 binary pairs having separations  $> 3$  pc. The dark grey histogram are pairs matched between TGAS stars while the red histogram denotes stars matched between TGAS and SDSS. The light grey histogram is the combined sample.

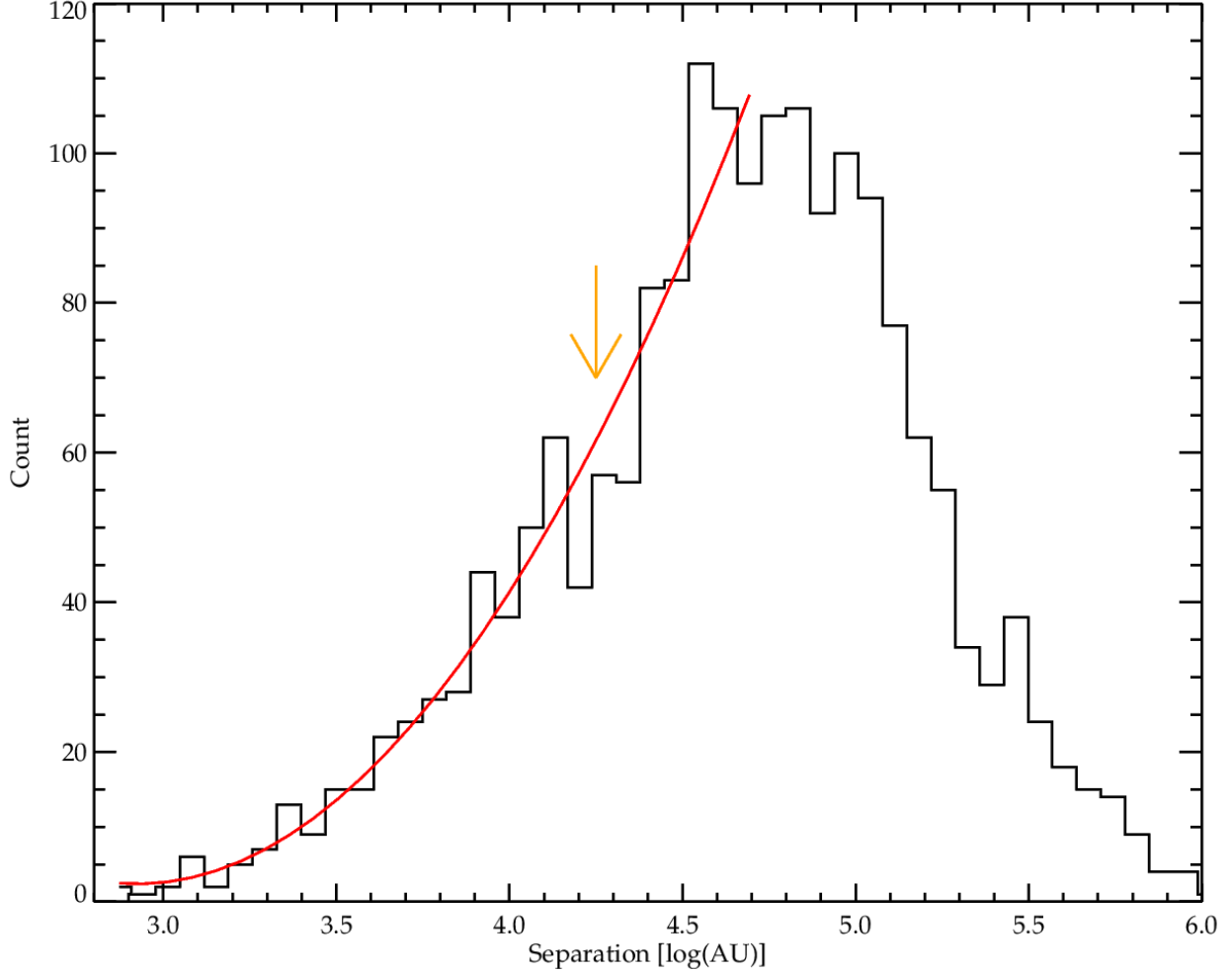


Fig. 5.— The full distribution of GAMBLEs binaries as a function of projected separation in  $\log[\text{AU}]$ . The split in the bimodal distribution of the TGAS-SDSS sample is marked by the orange arrow. The slight dip in the number of pairs could signify a trend with dissipation lifetime, as discussed in §6. Given the binaries in the TGAS-TGAS sample are dominated by higher-mass objects, the well-fit single power law could suggest higher mass stars prefer a single type of wide binary formation.

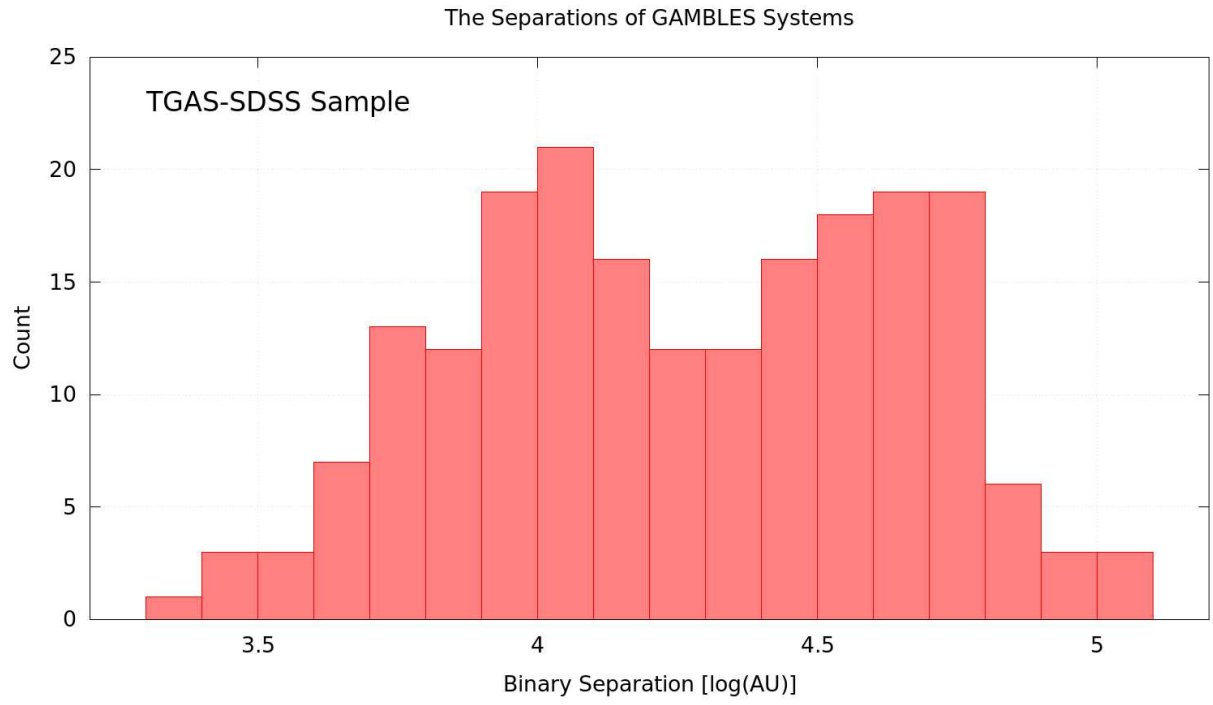


Fig. 6.— The projected separation for GAMBLES binaries in the TGAS-SDSS sample in  $\log(\text{AU})$  (*bottom*). A clear bimodal distribution is seen with peaks at  $\sim 10^{4.1}$  and  $\sim 10^{4.75}$  AU corroborating previous SLoWPoKES work.

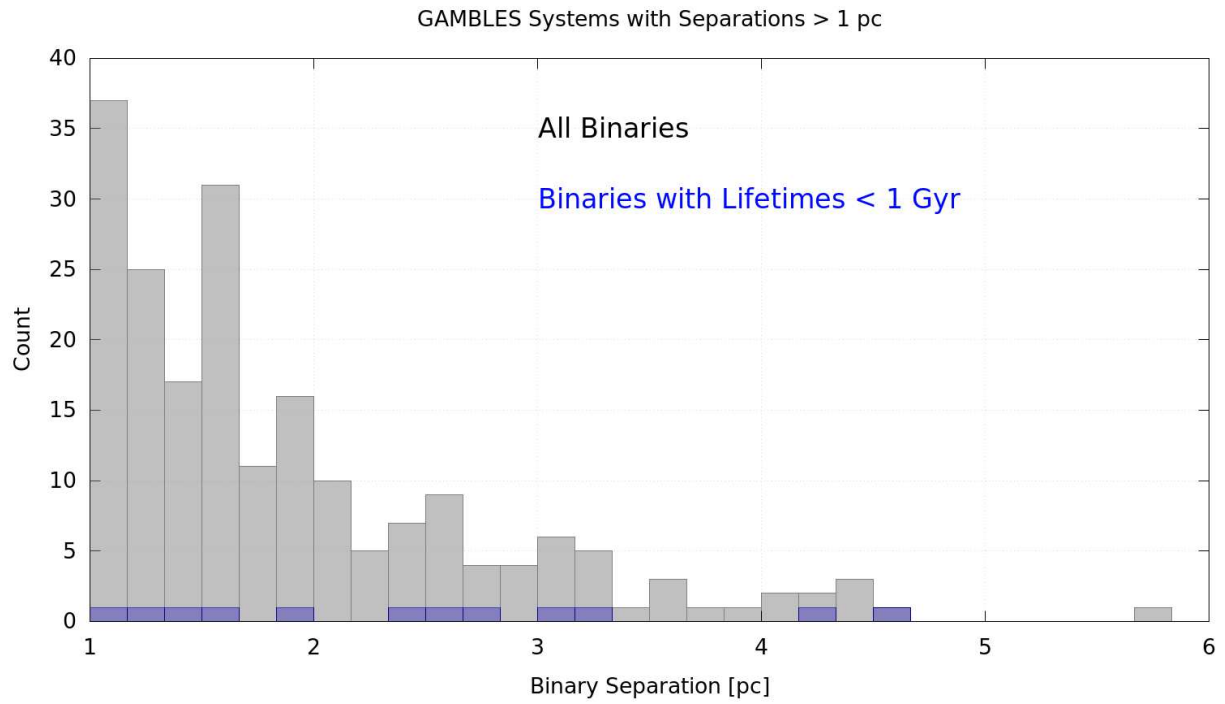


Fig. 7.— The projected separation for very-wide binaries in the GAMBLES sample. We find 248 binaries to have separations of 1 or more parsecs, with the largest separation being at  $\sim 5.76$  pc. The total sample is shown in dark grey. The blue histograms show the binaries with dissipation lifetimes shorter than 1 Gyr.

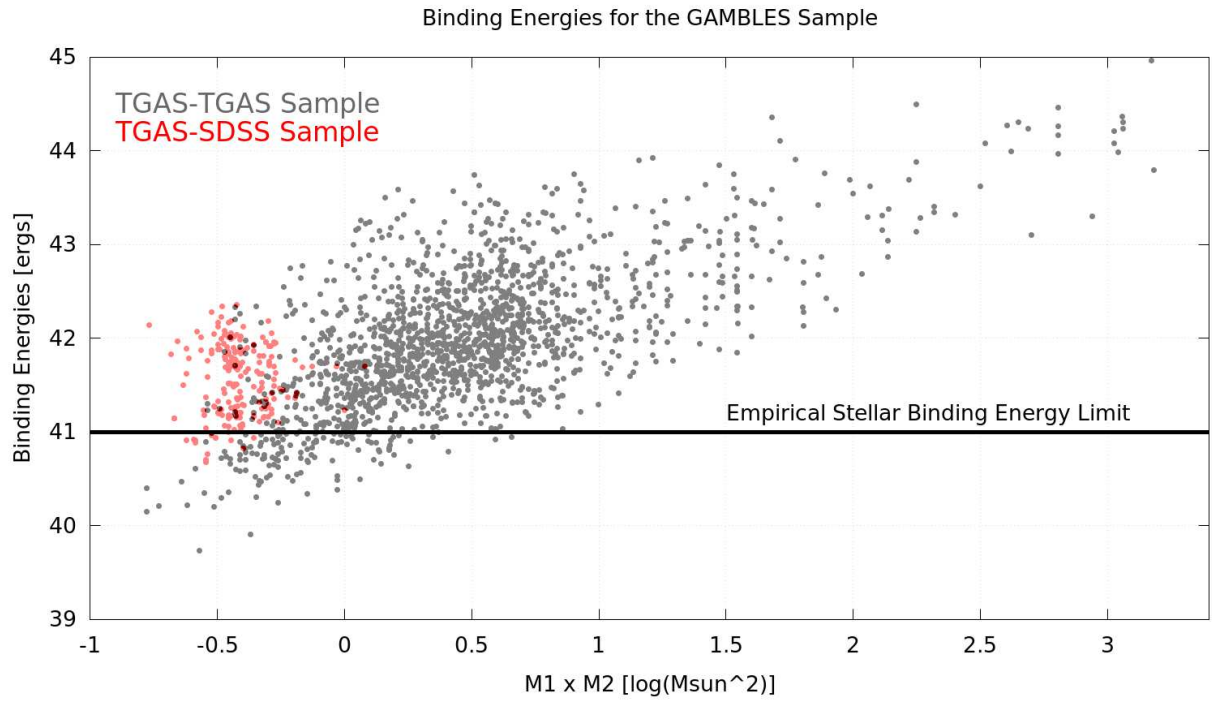


Fig. 8.— The binding energies of GAMBLES binaries (black dots) as a function of product of component masses. The red dots mark the pairs from the TGAS-SDSS sample and the black dots mark the pairs from the TGAS-TGAS sample. The solid black line denotes an empirical cutoff of  $10^{41}$  ergs as suggested from (Close et al. 2003, 2007).

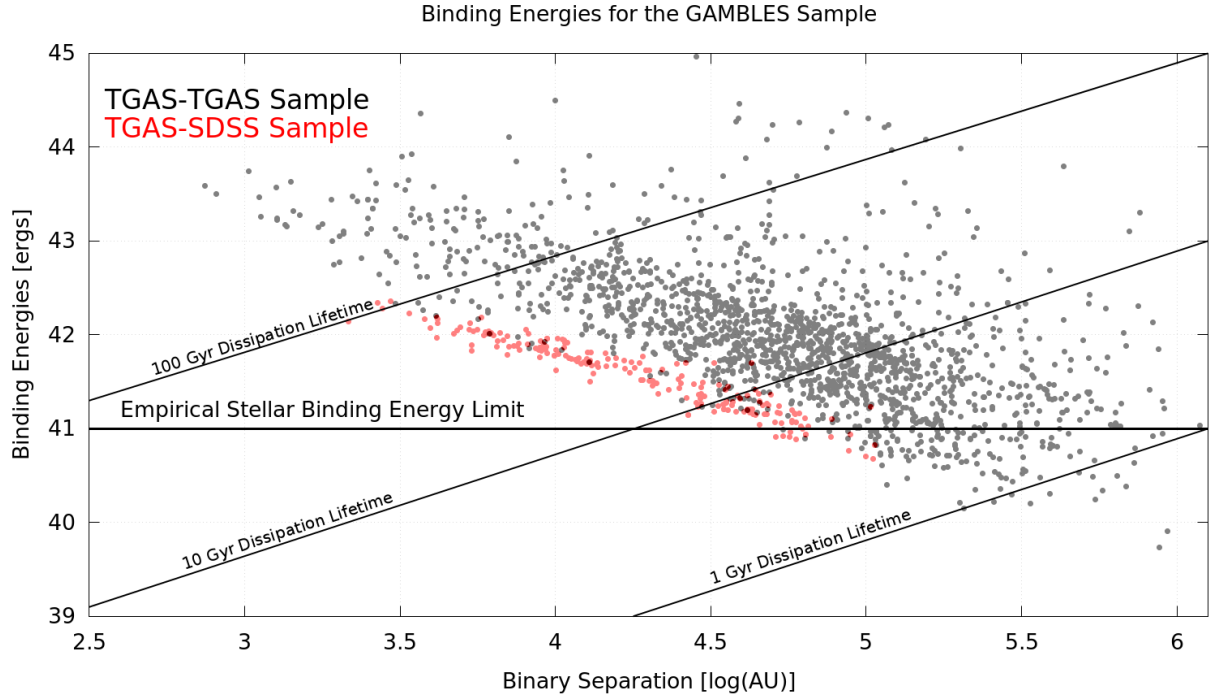


Fig. 9.— The separation for GAMBLES binaries and each binary pair’s calculated binding energy. The binaries from the TGAS-SDSS sample are marked with red dots while the binaries from the TGAS-TGAS sample are marked with black dots. The diagonal lines mark the approximate dissipation timescales of 1, 10 and 100 Gyr. We see that nearly every pair in the GAMBLES sample has an expected gravitationally stable lifetime of  $> 1$  Gyr, with only 10 objects ( $\sim 1\%$ ) having dissipation lifetimes  $< 1$  Gyr.

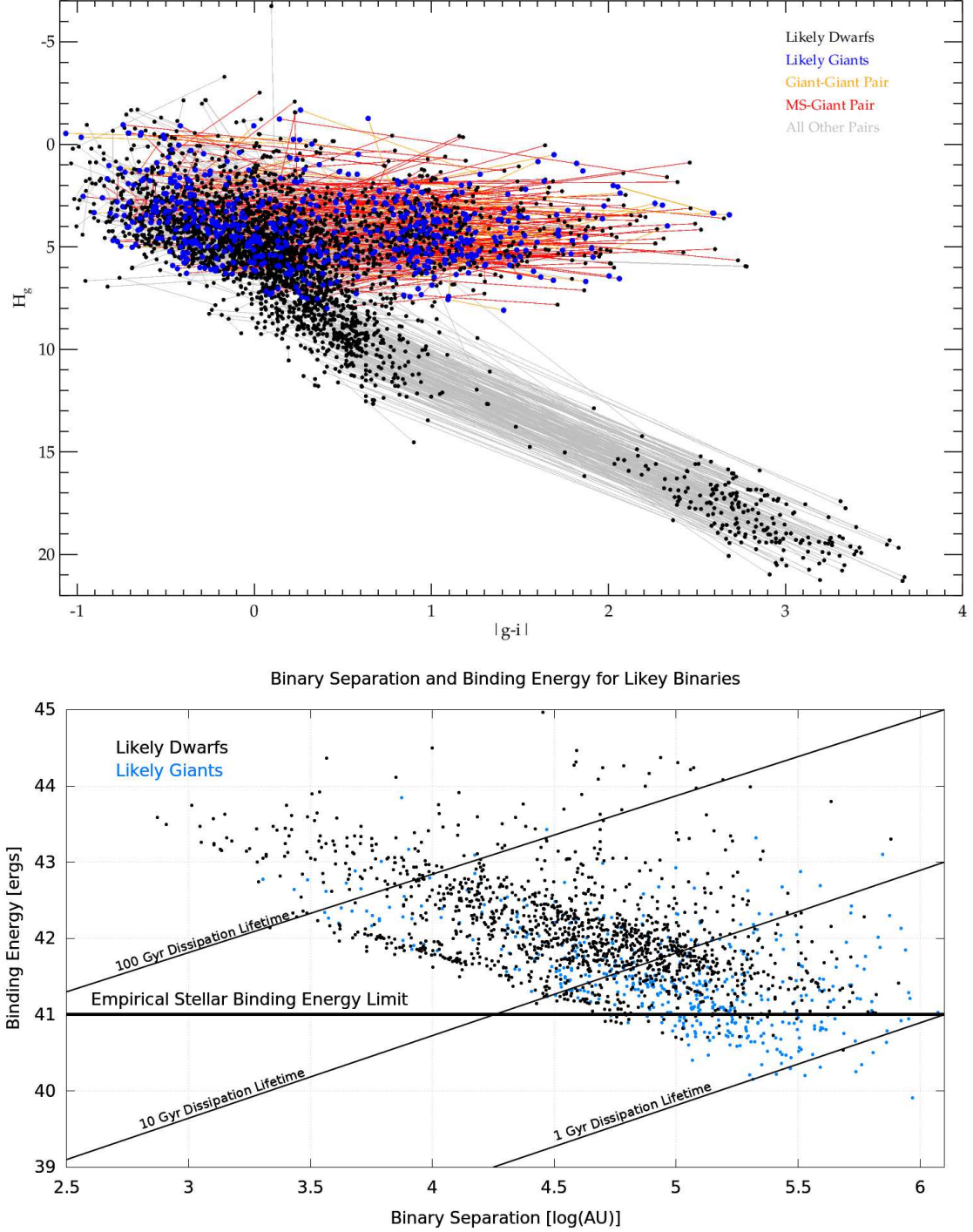


Fig. 10.— (*top*:) The reduced proper motion diagrams for GAMBLEs binaries in  $g$  used to identify possible giants. Using the relations from Casagrande et al. (2010) and the *Gaia* distances, the radius of the TGAS stars were estimated. Any star with a radius  $> 10R_{\odot}$  was flagged as a possible giant (blue dots) main sequence dwarfs are black dots. The lines denote matching pairs with grey lines matching between MS stars, orange lines matching between MS and Giant stars and red lines matching between giant pairs. (*Bottom*:) The binding energies of GAMBLEs binaries with at least 1 suspected giant component (blue dots). These binding energies should be treated as upper limits.

Table 1. GAMBLES Candidate Wide Binaries

ID	$\alpha_1$	Coordinates [deg]		$\delta_2$	Separation		$\Theta$	Spectral Type		Binding Energy	Lifetime	$V_5$	Class	Sample
		$\delta_1$	$\alpha_2$		pc	AU	[ $''$ ]			[log(ergs)]	[Gyr]			
GBL0141+0034	25.363768	0.575394	25.391928	0.577507	0.205	42381.34	101.65	F9	M3	41.207	1.43	0.001	MS+SDM	SDSS
GBL1150+0529	177.605698	5.483979	177.593094	5.501985	0.057	11745.72	79.00	G3	M3	41.720	1.33	0.001	MS+SDM	SDSS
GBL2108+1823	317.143036	18.390104	317.107880	18.396643	0.247	50973.96	122.37	G4	M3	41.069	1.30	0.015	MS+SDM	SDSS
GBL2236+1506	322.640839	19.489408	322.592621	19.439669	0.226	46556.26	107.85	F3	M4	41.253	1.73	0.003	MS+SDM	SDSS
GBL2337+1956	339.194733	15.109851	339.225647	15.107150	0.309	63809.30	172.37	G8	M2	40.935	1.20	0.001	MS+MS	SDSS
GBL2337+2135	354.418732	19.945599	354.446899	19.985483	0.280	57853.67	174.85	F4	M2	41.198	1.74	0.001	MS+SDM	SDSS
GBL0803+2435	354.462646	21.595364	354.440735	21.639456	0.046	9413.50	52.65	F4	M3	41.963	1.72	0.001	MS+MS	SDSS
GBL1037+2307	120.989349	24.593361	120.996025	24.580053	0.036	7518.02	32.41	G7	M2	41.880	1.23	0.001	MS+SDM	SDSS
GBL0942+4440	145.512604	28.877249	145.539597	28.926346	0.169	34881.08	135.57	G6	M3	41.205	1.24	0.001	MS+MS	SDSS
GBL0935+4616	145.608536	44.682056	145.643265	44.710487	0.066	13649.47	44.09	F9	M3	41.699	1.43	0.001	MS+SDM	SDSS
GBL1752+1434	197.036789	-1.975289	197.039780	-1.979283	0.212	43814.70	41.24	A5	A4	42.209	4.01	0.001	MS+MS	TGAS
GBL1756+1140	224.960602	-3.119409	224.911987	-3.126816	0.594	122567.14	114.82	A8	A8	41.654	3.54	0.030	MS+MS	TGAS
GBL1804+1119	222.225174	-7.159275	222.224213	-7.152433	0.409	84412.81	67.98	A1	F4	41.825	3.71	0.007	MS+MS	TGAS
GBL1752+1435	306.995819	-0.723825	307.000641	-0.738258	0.212	43814.70	41.24	A4	A5	42.209	4.01	0.001	MS+MS	TGAS
GBL1840+0907	338.564575	-7.254865	338.611725	-7.245229	0.115	23660.02	17.94	G1	B7	42.498	5.13	0.004	MS+MS	TGAS
GBL1840+1356	269.172119	11.673241	269.177063	11.641713	0.197	40651.06	62.44	F2	F7	41.851	2.58	0.021	MS+MS	TGAS
GBL1840+1356	271.158630	11.322003	271.176300	11.329507	0.197	40651.06	62.44	F6	F1	41.907	2.74	0.033	MS+MS	TGAS
GBL1903+1440	283.397858	9.749613	283.418121	9.737101	0.279	57560.38	39.46	A6	A7	42.039	3.78	0.047	MS+MS	TGAS
GBL1914+1334	276.374817	13.012628	276.360260	13.049245	0.017	3566.79	13.89	G8	F5	42.732	2.15	0.001	MS+MS	TGAS
GBL1927+0916	279.642426	11.942321	279.669403	11.973296	0.013	2588.39	18.02	A9	A6	43.342	3.60	0.001	MS+MS	TGAS
GBL1926+0916	279.669403	11.973296	279.642426	11.942321	0.013	2588.39	18.02	A6	A9	43.342	3.60	0.001	MS+MS	TGAS

Note. — \*: This is only a part of the full table to be released online. The Class column designates the type of identified pair, i.e. MS+MS, MS+SDM, WD+WD etc. The Match column designates which sample the binaries were identified in, TGAS-TGAS as TGAS or TGAS-SDSS as SDSS.